

Characterization of H-plasma treated ZnO crystals by positron annihilation and atomic force microscopy

J. Čížek^{1a}, I. Procházka¹, J. Kuriplach¹, W. Anwand², G. Brauer²,
T.E. Cowan², D. Grambole³, H. Schmidt³ and W. Skorupa³

¹Faculty of Mathematics and Physics, Charles University in Prague,
V Holešovičkách 2, CZ-18000 Praha 8, Czech Republic

²Institut für Strahlenphysik, Helmholtz-Zentrum Dresden-Rossendorf,
PO Box 510 119, D-01314 Dresden, Germany

³Institut für Ionenstrahlphysik und Materialforschung, Helmholtz-Zentrum Dresden-Rossendorf,
PO Box 510 119, D-01314 Dresden, Germany

^ajakub.cizek@mff.cuni.cz (corresponding author)

Keywords: Zinc oxide, hydrogen, positron annihilation, atomic force microscopy.

Abstract. Nominally undoped, hydrothermally grown ZnO single crystals have been investigated before and after exposure to remote H-plasma. Defect characterization has been made by two complementary techniques of positron annihilation: positron lifetime spectroscopy and coincidence Doppler broadening. The high-momentum parts of the annihilation photon momentum distribution have been calculated from first principles in order to assist in defect identification. The positron annihilation results are supplemented by Atomic Force Microscopy for characterization of the crystal surface. It was found that virgin ZnO crystal contains Zn-vacancies associated with hydrogen. H-plasma treatment causes a significant reduction in concentration of these complexes. Physical mechanism of this effect is discussed in the paper.

Introduction

Hydrothermally grown (HTG) ZnO single crystals were the subject of systematic studies by positron annihilation spectroscopy (PAS), in combination with theoretical calculations, in order to understand the role of native defects in ZnO [1-3]. Hydrogen - hereafter referred to as H - has been detected in Ref. [1] by nuclear reaction analysis (NRA) in all HTG ZnO crystals in a bound state with a high concentration (at least 0.3 at.-%), whereas the concentrations of other impurities are very small. Moreover, the presence of H in ZnO crystals was predicted by *ab-initio* theoretical calculations [4,5]. Comparison of recent *ab-initio* calculations with experimental PAS data suggested that HTG ZnO single crystals contain Zn-vacancy + hydrogen ($V_{Zn}+1H$) complexes [1]. However, the general role of H in ZnO is still far from being completely understood.

Further characterization of HTG ZnO single crystals was performed in the present work. HTG ZnO single crystals were subjected to remote H-plasma treatment and the effect of this treatment on the structure of ZnO crystals and point defects was characterized by PAS. Two complementary PAS techniques were employed to obtain a complex picture about defects in H-plasma treated crystals: (i) positron lifetime (LT) spectroscopy which enables to identify defects and to estimate defect densities and (ii) coincidence Doppler broadening (CDB) which carries information about local chemical environment of defects. Experimental PAS data were interpreted using *ab-initio* theoretical calculations of positron parameters. In the present work PAS studies were combined with characterization of H-plasma treatment-induced surface modifications by atomic force microscopy (AFM). This work is a continuation of previous investigations of H-plasma treated HTG ZnO single crystals by slow positron implantation spectroscopy (SPIS) combined with pulsed low energy positron spectroscopy (PLEPS) [6] and by Hall measurements combined with photoluminescence [7].

Experimental Details

Sample description and plasma treatment. HTG single crystals with (0001) orientation and O-face optically polished were supplied by MaTecK GmbH (Jülich) in 2008. The samples were firstly characterized in the virgin state and subsequently were exposed for 1 h to a remote H dc plasma in a parallel-plate system, with a plate voltage of 1000 V. Samples were mounted on a heater block held at a temperature of 350 °C placed ~ 100 mm downstream from the plasma with a bias voltage of -330 V, which fixed the bias current to ~ 50 μ A. During the loading the gas pressure was held at ~ 1 mbar. Subsequently, H-plasma treated crystals were characterized and compared with the virgin samples. The H content in ZnO crystals was determined by nuclear reaction analysis (NRA) [8] using 6.64 MeV ^{15}N ions. The H detection limit by NRA is ~ 200 ppm and H concentration is determined at a depth of ~ 100 nm, as estimated by SRIM ('The Stopping and Range of Ions in Matter' – software which describes the transport properties of ions in matter [9]). Hence the penetration depth of ^{15}N ions is high enough to guarantee that volume properties, without any influence of surface contaminations, are being studied.

Positron annihilation spectroscopy. A $^{22}\text{Na}_2\text{CO}_3$ positron source with an activity of ~ 1.5 MBq deposited on a ~ 2 μm thick mylar foil was used in PAS measurements. The source was always sandwiched between a pair of ZnO crystals. LT measurements were performed on a digital spectrometer described in Refs. [10,11]. The spectrometer is equipped with BaF_2 scintillators and fast photomultipliers Hamamatsu H3378. Detector pulses are directly digitized using a couple of 8-bit ultra-fast digitizers Acqiris DC 211 with sampling frequency of 4 GHz and stored in a PC. Analysis of digitized pulses and construction of LT spectrum is performed off-line using so called integral true constant fraction technique described in Ref. [12]. The spectrometer exhibits excellent time resolution of 145 ps (FWHM ^{22}Na). The LT spectra, which always contained at least 10^7 positron annihilation events, were decomposed using a maximum likelihood based procedure [13]. The source contribution to LT spectra consisted of two weak components with lifetimes of ~ 368 ps and ~ 1.5 ns and corresponding intensities of ~ 7 % and ~ 1 %.

CDB studies were carried out using a spectrometer [14] equipped with two high purity Ge detectors. The energy resolution of the CDB spectrometer is (1.00 ± 0.01) keV at 511 keV. At least 10^8 annihilation events were collected in each two-dimensional γ -ray energy spectrum, which was subsequently reduced into two one-dimensional cuts representing the resolution function of the spectrometer and the Doppler broadened annihilation profile. A well annealed pure Zn (99.99 %) was used as a reference specimen in CDB investigations.

Atomic force microscopy. The surface morphology of the ZnO single crystals was investigated by means of AFM measurements in the tapping mode using a Dimension DI 3100 from Veeco Instruments and rotated tapping mode etched silicon probes (RTESP) with a nominal tip radius < 10 nm.

Theoretical Calculations

Theoretical calculations of the high momentum part (HMP) of the momentum distribution of annihilation photons were performed in order to assist defect identification. Positron parameters were calculated from the first principles using an approach based on the density functional theory. Positron wave function was calculated using so called standard scheme described in Ref. [15]. The electron-positron correlation was treated within the generalized gradient approximation (GGA) scheme developed by Barbiellini [16]. In addition to the defect-free ZnO lattice, three defect configurations were considered: Zn vacancy (V_{Zn}) and two configurations of V_{Zn} with one H atom creating a bond with a neighboring O atom. The latter two configurations are labeled as ' $V_{\text{Zn}+1\text{H}}_{\text{ab}}$ ' and ' $V_{\text{Zn}+1\text{H}}_{\text{c}}$ ', where 'ab' and 'c' indicate, respectively, that the corresponding H-O bond has a non-zero projection to the 'ab' basal plane of the ZnO hexagonal lattice or that such a bond is oriented along the c-axis direction. Relaxed defect configurations were obtained using an *ab-initio* computational method - taking into account positron-induced forces [17] - and were taken from Ref. 1, where a more detailed description of considered defect geometry configurations can also be found.

Calculations of HMP's were carried out according to the scheme presented in Ref. 18. In the case of Zn, the core electron configuration was represented by that of an Ar atom plus ten $3d$ electrons. For O, the $1s^2 2s^2 2p^2$ core electron configuration gave the best agreement with experiment. One electron of H was also treated as a core electron, but this should only be considered as an attempt to evaluate possible H-related features in the HMP's of the CDB curves. More precise calculations would require a fully self-consistent treatment. Since valence electrons contributing predominantly to the low momentum region are not handled in our HMP calculations, the comparison of calculated and measured ratio profiles should be made only for the high momentum region $p > 10 \times 10^{-3} m_0c$ where the contribution of core electrons dominates (see Ref. 18 for details).

Results and Discussion

Positron lifetime spectroscopy. The virgin ZnO crystal exhibits a single LT component spectrum with lifetime of (180.6 ± 0.3) ps. This lifetime is significantly longer than the ZnO bulk positron lifetime of 154 ps [1] or 153 ps [19] obtained from *ab-initio* theoretical calculations. This testifies that the majority of positrons in the virgin ZnO crystal annihilates from a trapped state at defects. The nature of these defects was disclosed in Ref. 1 where it was shown that the lifetime measured in a virgin HTG ZnO crystal is comparable with the lifetime of 179 ps and 177 ps calculated for positrons trapped in V_{Zn+1H_ab} and V_{Zn+1H_c} complex, respectively. This result corresponds well with a significant concentration of H impurities amounting 0.3 at.-% determined in the virgin HTG ZnO crystal by NRA. Since lifetimes corresponding to the two configurations of V_{Zn+1H} complexes are very close to each other, it is not possible to distinguish them by LT spectroscopy.

Contrary to the virgin sample, the H-plasma treated ZnO crystal exhibits a two component LT spectrum consisting of a short-lived component with lifetime $\tau_1 = (50 \pm 10)$ ps and relative intensity $I_1 = (6 \pm 1) \%$ and a long-lived component with lifetime $\tau_2 = (175.9 \pm 0.5)$ ps and relative intensity $I_2 = (94 \pm 1) \%$. The latter component clearly represents a contribution of positrons trapped at V_{Zn+1H} complexes while the short-lived component comes from free positrons which are not trapped at defects. The bulk positron lifetime

$$\tau_B = \left(\frac{I_1}{\tau_1} + \frac{I_2}{\tau_2} \right)^{-1} \quad (1)$$

calculated using the two state trapping model [20] is (153 ± 3) ps, which is in excellent agreement with the calculated bulk lifetime in ZnO [1,19]. Interestingly very similar value of the bulk lifetime (151 ± 2) ps was obtained by application of the two state trapping model on electron irradiated ZnO crystal [21]. This result is remarkable because there is still controversy about the correct value of ZnO bulk lifetime. The single component with lifetime 180-185 ps found in the virgin HTG ZnO crystals was interpreted as 'bulk lifetime' in some papers [2,3] despite the fact that it is significantly longer than the bulk ZnO lifetime obtained from *ab-initio* theoretical calculations and positron diffusion length in virgin HTG ZnO crystals determined by SPIS is very short indicating existence of open-volume defect which trap positrons.

In our very comprehensive paper [1] we have extensively discussed the issue of the 'true bulk lifetime' of ZnO. As a result of these discussions, we arrived at the conclusion that ~ 153 ps is the almost correct value. In HTG ZnO crystals positrons annihilate from trapped state at V_{Zn+1H} complexes which gives lifetime of ~ 180 ps. Saturation positron trapping at defects characterized by a shorter lifetime of ~ 163 ps was found also in melt grown ZnO. In a recent paper [22] these defects were identified as stacking faults.

Our results in this work support the picture drawn in Ref. [1] that positrons in HTG ZnO crystals are trapped at $V_{Zn}+1H$ complexes. In HTG ZnO crystals H is easily incorporated into the sample during the crystal growth. The presence of H reduces the formation energy of V_{Zn} due to positive binding energy of H to V_{Zn} which is released when $V_{Zn}+1H$ complex is formed. Due to this reason it is very difficult to prepare a HTG ZnO crystal without $V_{Zn}+1H$ complexes. In this context it is interesting that H-plasma treatment causes a significant decrease in the density of positron traps, i.e. $V_{Zn}+1H$ complexes, in HTG ZnO crystals.

Since the free positron contribution was detected in LT spectrum of H-plasma treated crystal the two state trapping model [20] can be used to estimate the concentration of $V_{Zn}+1H$ complexes

$$c_{v_{Zn}+1H} = \frac{I_2}{\nu_v} \left(\frac{1}{\tau_1} - \frac{1}{\tau_2} \right), \quad (2)$$

where ν_v is the specific positron trapping rate to $V_{Zn}+1H$ complexes. Assuming $\nu_v = 1 \times 10^{15} \text{ s}^{-1}$ which is a typical value for neutral vacancies in semiconductors [23], the concentration of $V_{Zn}+1H$ complexes obtained from Eq. (2) is $c_{v_{Zn}+1H} \approx 1.3 \times 10^{-5} \text{ at.}^{-1}$ ($1.1 \times 10^{18} \text{ cm}^{-3}$). Note that volume concentration in bracket is the atomic concentration multiplied by $N_A \rho / M$, where N_A is the Avogadro constant, $\rho = 5.606 \text{ gcm}^{-3}$ is the ZnO density and $M = 1/2 (M_O + M_{Zn})$ is the average molar mass of Zn and O.

The concentration of $V_{Zn}+1H$ complexes in the virgin HTG ZnO crystal cannot be calculated from LT data due to saturated positron trapping, but it can be estimated from the positron diffusion length determined by SPIS

$$c_{v_{Zn}+1H} = \frac{1}{\nu_v \tau_B} \left(\frac{L_{+,B}^2}{L_+^2} - 1 \right). \quad (3)$$

Here $L_{+,B}$ and L_+ is the mean positron diffusion length in a perfect (defect-free) ZnO and in the virgin HTG ZnO crystal, respectively. The positron diffusion length $L_+ = (38 \pm 11) \text{ nm}$ [6] was determined in HTG ZnO crystal by SPIS. Taking into account the uncertainty of L_+ this value is comparable with positron diffusion length of around 50 nm determined for ZnO crystals in Refs. [24-27] and is significantly shorter than $\sim 200 \text{ nm}$ which is a typical value for defect-free semiconductors, e.g. Si [28] and GaAs [29]. This testifies that ZnO crystals contain a significant concentration of open volume defects. Hence using $L_{+,B} \approx 200 \text{ nm}$ and $\tau_B = 154 \text{ ps}$, the concentration of $V_{Zn}+1H$ complexes in the virgin HTG ZnO crystal estimated by Eq. (3) is $c_{v_{Zn}+1H} \approx 2 \times 10^{-4} \text{ at.}^{-1}$ ($1 \times 10^{19} \text{ cm}^{-3}$). Thus, H-plasma treatment leads to a decrease in the density of $V_{Zn}+1H$ complexes at least by one order of magnitude.

Note that it is very difficult to resolve the free positron component in a LT spectrum when $I_f < 5\%$. To make a conservative estimation, the free positron component certainly cannot be resolved when its intensity approaches $\approx 1\%$. Using the two-state trapping model one can estimate that saturated positron trapping occurs when concentration of $V_{Zn}+1H$ complexes exceeds $\approx 0.8 \times 10^{-4} \text{ at.}^{-1}$ ($0.7 \times 10^{19} \text{ cm}^{-3}$). This is in accordance with the concentration of $V_{Zn}+1H$ complexes in the virgin HTG ZnO crystal estimated by Eq. (3).

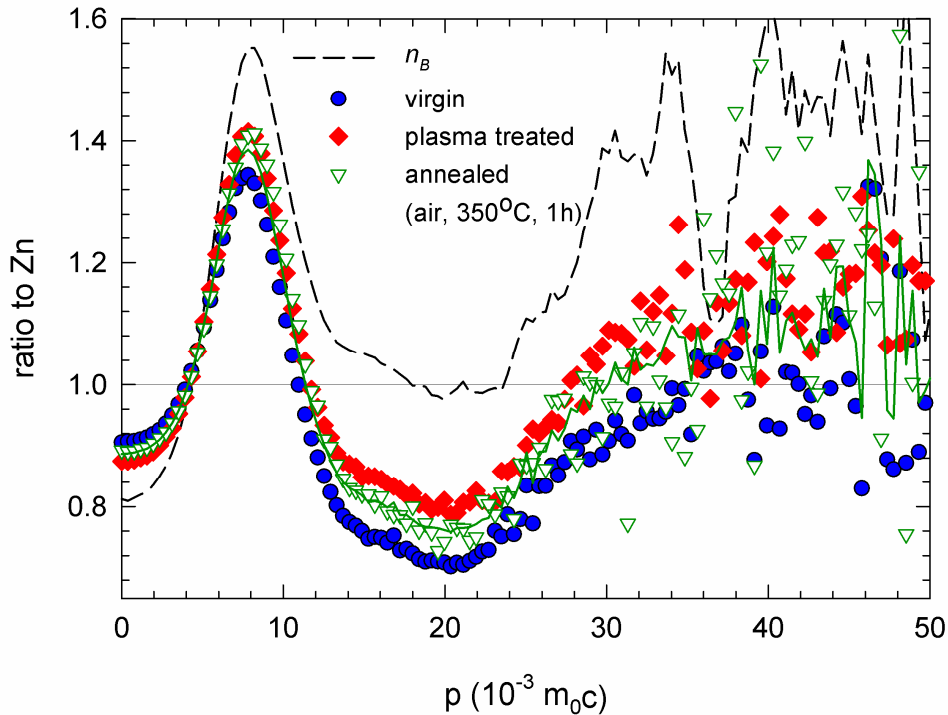


Figure 1 Experimental CDB ratio curves (related to the pure Zn reference sample). Dashed line shows estimated momentum distribution of electrons which annihilated free positron in ZnO.

Coincidence Doppler broadening. Fig. 1 shows results of CDB measurements presented as ratio curves (i.e., relative to the well-annealed pure Zn reference sample). The ratio curve measured on the virgin ZnO crystal exhibits certain characteristic features. A sharp maximum which can be observed at $p \approx 8 \times 10^{-3} m_0c$ is due to a contribution of positrons annihilated by $2p$ O electrons. The absence of a $3d$ electron contribution for positrons annihilated by O electrons causes the appearance of a broad minimum at $p \approx 20 \times 10^{-3} m_0c$. The broad peak in the region $p \approx 35-45 \times 10^{-3} m_0c$ is due to the contribution of $2s$ O electrons.

Theoretically calculated ratio curves (related to a perfect hcp Zn crystal) are plotted in Fig. 2. The calculated HMP curves compare well qualitatively with experiment regarding the position of the maximum ($8 \times 10^{-3} m_0c$) and minimum ($20 \times 10^{-3} m_0c$) followed by a broad peak ($35-45 \times 10^{-3} m_0c$). Although on the vertical scale the absolute position of the calculated profiles is not precise enough for a quantitative comparison with experiment, these profiles still can give a qualitative description of the behavior of CDB curves for various positrons states, which makes them useful for an interpretation of the experimental data.

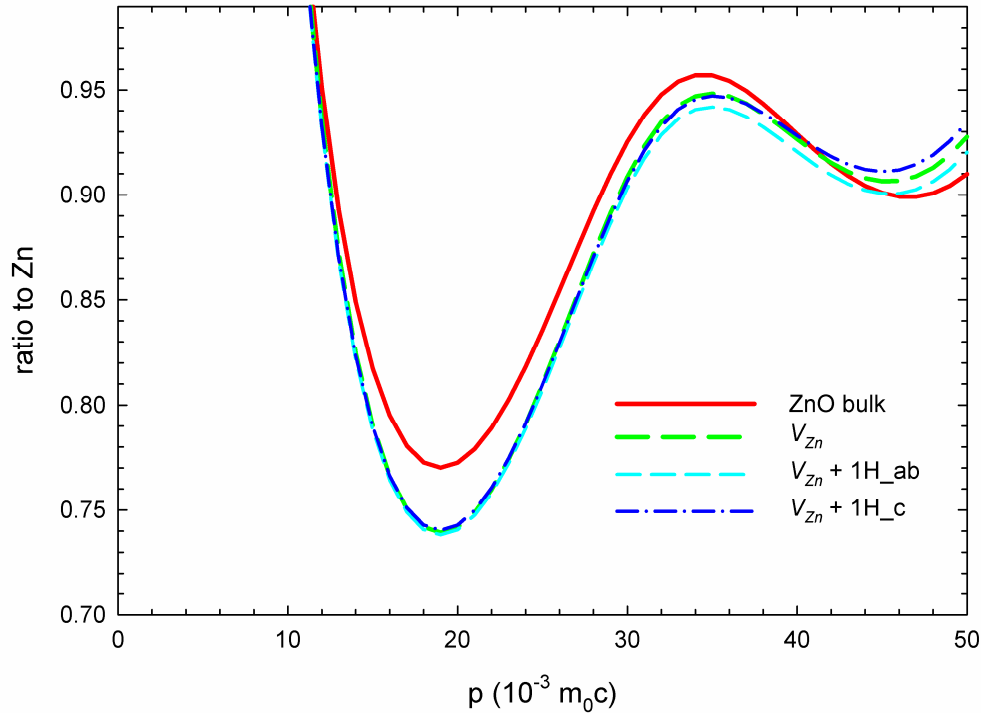


Figure 2 Calculated HMP ratio profiles for bulk ZnO and various defects. All curves are related to a perfect hcp Zn crystal.

One can see in Fig. 2 that the calculated curve for free positrons in a perfect ZnO crystal is located above the curves calculated for V_{Zn} and its complexes with H. Hence, free positrons contribute to the high momentum range ($p > 10 \times 10^{-3} m_0c$) more than positrons trapped at defects. This happens because the wave function of a trapped positron is localized in a defect and its overlap with high-momentum core electrons is lowered compared to a free positron. Moreover, the minimum at $p \approx 20 \times 10^{-3} m_0c$ is more pronounced in the curves calculated for various V_{Zn} -related defects and less pronounced in the curve for perfect ZnO crystal. This reflects the fact that V_{Zn} is surrounded by nearest neighbor O anions. Hence, a positron trapped in a V_{Zn} -related defect annihilates predominantly with O electrons, while a free positron in ZnO is annihilated also by Zn electrons. The calculated profiles do not differentiate clearly between the various defects studied. This is probably due to the fact that H possesses only one electron and that such an electron can influence the ZnO CDB profile predominantly in the low momentum region ($p < 10 \times 10^{-3} m_0c$), which is not treated accurately in our calculations. We might thus conclude that despite of a good qualitative agreement of HMP profiles with measurements, any more precise defect identification based on CDB profiles is not possible at this stage of research.

The CDB ratio curve measured for an H-plasma treated crystal exhibits similar features as that for the virgin crystal, but it is enhanced in the high momentum region $p > 5 \times 10^{-3} m_0c$ and lowered at low momenta $p < 5 \times 10^{-3} m_0c$. From an inspection of Fig. 1 one can deduce that the enhancement in the high momentum region is basically uniform - i.e. the whole curve at high momenta is simply shifted up. In order to see exclusively the effect of H-plasma treatment on CDB results, Fig. 3 shows CDB ratio curves relative to the virgin ZnO crystal. One can see in Fig. 3 that the ratio curve for an H-plasma treated crystal is enhanced (i.e. higher than 1) and rather flat over the whole high momentum range. This testifies that the chemical environment of positron annihilation sites remains basically unchanged, but the fraction of positrons trapped at defects was reduced in the H-plasma treated crystal. This agrees well with results from LT measurements which revealed a free positron component in the H-plasma treated crystal, while the virgin crystal exhibited saturated positron trapping in defects.

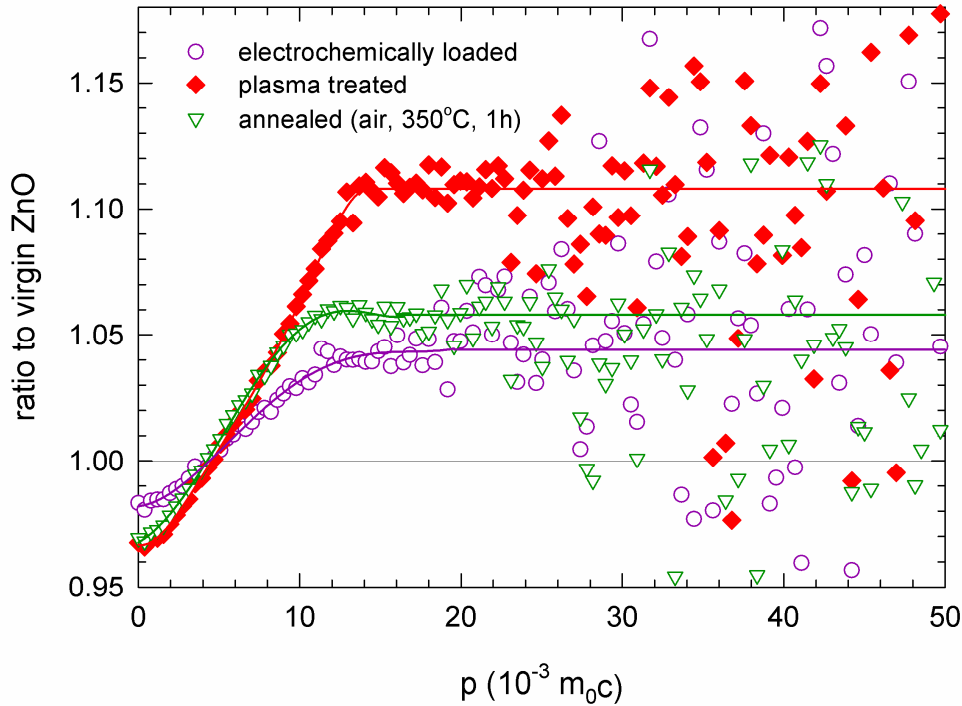


Figure 3 CDB results of differently treated HTG ZnO single crystals related to a virgin ZnO crystal. Solid lines are intended just to guide eyes

The momentum distribution of annihilating electron-positron pairs in the H-plasma treated crystal can be expressed as

$$n = F_B n_B + F_D n_D, \quad (4)$$

where n_B and n_D denote the momentum distribution of electrons which annihilated free positrons delocalized in ZnO crystal and positrons trapped in defects (i.e. $V_{Zn}+1H$ complexes). The symbol F_D denotes the fraction of positrons trapped in $V_{Zn}+1H$ complexes, while the fraction of positrons annihilated in the free state is $F_B = 1 - F_D$. The fraction of positrons trapped in $V_{Zn}+1H$ complexes can be determined from LT results

$$F_D = \frac{\tau_B K}{1 + \tau_B K}, \quad (5)$$

where K is the positron trapping rate into $V_{Zn}+1H$ complexes

$$K = \frac{I_2}{I_1} \left(\frac{1}{\tau_B} - \frac{1}{\tau_2} \right). \quad (6)$$

From Eqs. (5-6) one obtains the fraction of positrons trapped in $V_{Zn}+1H$ complexes in the H-plasma treated crystal $F_D = 0.67 \pm 0.05$, while in the virgin crystal virtually all positrons are trapped, i.e. $F_D \approx 1$. Thus, the momentum distribution measured in the virgin crystal approximately equals n_D . The momentum distribution of electrons which annihilated free positrons in ZnO can be obtained from a combination of LT and CDB results as

$$n_B = \frac{n - F_D n_D}{1 - F_D}. \quad (7)$$

The momentum distribution n_B obtained from Eq. (7) is plotted in Fig. 1 as a dashed line. Although there is a significant difference in the vertical position of calculated HMP profiles and experimental curves, the features predicted in theoretical calculations can be qualitatively seen in experimental data. Namely, one can see in Fig. 1 that n_B exhibits: (i) enhanced contribution of positrons annihilated by O electrons, which is reflected by increased peak at $p \approx 8 \times 10^{-3} m_0c$, and (ii) overall uniform enhancement in the high momentum region accompanied by a drop at the low momenta due to increased overlap of positron wave function with core electrons.

Hence, CDB spectroscopy supports the picture drawn from LT measurements and gives additional and independent evidence that the concentration of positron traps was lowered in the volume of the H-plasma treated crystals. This is demonstrated by detectable fraction of positrons annihilating from the free state. This picture is further supported by SPIS investigations which revealed an increase of positron diffusion length in H-plasma treated crystal [6].

The similar shapes of the CDB ratio curves for the virgin and H-plasma treated crystals indicate that the nature of positron traps in these samples remains essentially the same - only their density was lowered in the H-plasma treated crystal. A decrease in the density of positron traps in the H-plasma treated crystal can be caused by several processes:

(i) *thermally activated mutual annihilation of $V_{Zn}+1H$ complexes with Zn interstitials (Zn_i)*. Since the sample is kept at a temperature of 350°C for 1h during the H-plasma treatment, the concentration of positron traps may be reduced due to thermally-induced recovery. Zn_i , which may exist in the crystal, become mobile at temperatures above ~200 °C [30,31] and may fill up some of the existing $V_{Zn}+1H$ complexes. In this way V_{Zn} are no longer available for positron trapping. This could explain the observed decrease in the concentration of positron traps in a H-plasma treated ZnO crystal. The presence of Zn_i in the virgin ZnO crystal is reliably concluded from photoluminescence and Hall measurements [7].

(ii) *H-plasma assisted diffusion of Zn_i into the bulk and filling the $V_{Zn}+1H$ complexes*. SPIS and PLEPS investigations of H-plasma treated ZnO crystal revealed the formation of nanovoids in a sub-surface layer with a depth of 650 nm [6]. Comparison with theoretical calculations revealed that lifetime of these defects is comparable to a cluster of 4-6 Zn-O di-vacancies [6]. Nanovoid formation in H-plasma treated ZnO has been reported also in Ref 19. From μ -Raman spectroscopy it has been concluded that these nanovoids are created by coalescence of oxygen vacancies and should be filled with H_2 . Hence there is a loss of oxygen in a sub-surface region caused by H-plasma treatment. Since O atoms leave the sample during H-plasma treatment, the remaining Zn atoms diffuse as Zn_i and may fill existing $V_{Zn}+1H$ complexes. At the same time, H that is in the neighborhood may help in nucleation of such voids.

(iii) *trapping of H atoms into $V_{Zn}+1H$ complexes*. H atoms introduced into a ZnO crystal by H-plasma treatment are attached to $V_{Zn}+1H$ and convert them into $V_{Zn}+nH$ ($n \geq 2$) complexes. *Ab-initio* theoretical calculations by Karazhanov et al. [32] have shown that there is a positive binding energy of additional H to a $V_{Zn}+1H$ complex. H interstitials tend to fill all four bond-centered sites around a V_{Zn} forming a $V_{Zn}+4H$ complex. Recent theoretical calculations [1] have also shown that contrary to V_{Zn} and $V_{Zn}+1H$ defects, $V_{Zn}+nH$ ($n \geq 2$) complexes are too shallow potential wells to form a localized positron state. Hence, if some fraction of $V_{Zn}+1H$ existing in the virgin crystal is converted into $V_{Zn}+nH$ ($n \geq 2$) complexes, then the number of available positron traps is reduced.

To simulate thermal conditions during the H-plasma treatment and to examine if the process (i) may influence concentration of positron traps a virgin ZnO crystal was annealed at 350°C for 1h and examined by LT and CDB spectroscopy. LT investigations revealed a single component spectrum with a lifetime (177.9 ± 0.2) ps which is only slightly shorter than the lifetime measured in the virgin crystal and testifies saturated positron trapping in $V_{Zn}+1H$ complexes. The CDB ratio curve measured on the annealed crystal is plotted in Fig. 1 (relative to pure Zn) and in Fig. 3 (relative to virgin ZnO). One can see in Fig. 1 that compared to the curve for the virgin crystal the curve for the annealed crystal is higher in the high momentum region and lower in the low momentum region. Fig. 2 shows that the enhancement in the high momentum region is rather flat, i.e. very similar in shape to that observed in the H-plasma treated crystal but smaller in magnitude.

This result testifies that some thermally activated recovery of $V_{Zn}+1H$ complexes indeed occurred due to the elevated temperature during the H-plasma treatment. However, the results obtained in the annealed crystal testify also that the annealing itself is not able to explain fully the decrease in concentration of positron traps observed in the H-plasma treated crystal. Obviously H-plasma treatment assisted processes (ii) and/or (iii) take place as well and cause a stronger reduction in concentration of positron traps in the H-plasma treated crystal compared to the annealed sample. The momentum distribution in the annealed sample can be described by Eq (4). The solid line in Fig. 1 shows a best fit of experimental points by a linear combination of the momentum distributions n_B and n_D . The fit using Eq. (4) describes well the experimental points for the annealed crystal. The fraction of positrons annihilated in defects $F_D = (0.80 \pm 0.05)$ was obtained from fitting. Using Eq. (5) one can calculate that positron trapping rate to defects in the annealed crystal is rather high $K = (2.6 \pm 0.2) \times 10^{10} \text{ s}^{-1}$. From this one can deduce using Eq. (6) that the intensity of the free positron component in the annealed crystal is only 3 %. Since it is very difficult to resolve the free-positron component when $I_f < 5 \%$, it is not surprising that LT investigations of the annealed crystal revealed saturated positron trapping at defects.

Hence, one can conclude that although thermally activated annihilation of $V_{Zn}+1H$ and Zn_i is responsible for some reduction in the density of positron traps, it cannot fully explain the effect observed in the H-plasma treated crystals. The decrease in concentration of positron traps in the H-plasma treated crystal is higher than in the crystal which was only annealed. H-plasma assisted processes (ii) and (iii), therefore, cause a further reduction in the density of positron traps.

The process (iii) was studied separately in Ref. 33, where a ZnO crystal was electrochemically charged with hydrogen at room temperature. Using NRA it was found that a high hydrogen concentration of $\approx 0.30 \text{ at.}^{-1}$ was introduced into the crystal by electrochemical charging. LT investigations of the charged crystal revealed a single component spectrum with a lifetime of $(178.8 \pm 0.4) \text{ ps}$ [33] which indicates saturated positron trapping at $V_{Zn}+1H$ defects. The CDB ratio curve (related to the virgin ZnO crystal) measured on the charged crystal is plotted in Fig. 3. Interestingly, it exhibits a shape very similar to the curve obtained for the H-plasma treated and the annealed crystal - i.e., a uniform enhancement in the high momentum range and a decrease in the low momentum range. The magnitude of this effect is lower than in the H-plasma treated crystal but comparable with that in the annealed sample. This indicates that the process (iii) does take place in H-loaded ZnO.

In summary, it has been demonstrated that both processes (i) and (iii) cause a reduction in density of positron traps and have both a very similar effect on CDB spectra. The annealed crystal, where only the process (i) takes place, and the electrochemically charged sample, where only the process (iii) occurs, both exhibit LT spectra with a single component only (saturated positron trapping) and comparable enhancement in the high momentum part of CDB curves which is smaller than the enhancement observed in the H-plasma treated crystal. This strongly indicates that in H-plasma treated crystal both processes (i) and (iii) occur simultaneously, leading to a stronger reduction in the concentration of positron traps as demonstrated by the largest enhancement of the CDB curve in the high momentum region and appearance of the free-positron component in the LT spectrum. At the present stage of research one cannot exclude that a certain reduction in defect density occurs also due to the process (ii). However, it is difficult to examine this effect separately.

An H concentration of $(0.15 \pm 0.03) \times 10^{-2} \text{ at.}^{-1}$, i.e. $(1.2 \pm 0.3) \times 10^{20} \text{ cm}^{-3}$, was found at a depth of 600 nm in the H-plasma treated crystal by NRA investigations. This is comparable to an H concentration of $(0.14 \pm 0.03) \times 10^{-2} \text{ at.}^{-1}$, i.e. $(1.1 \pm 0.3) \times 10^{20} \text{ cm}^{-3}$, determined in the virgin crystal. An enhanced H concentration of $(0.58 \pm 0.09) \times 10^{-2} \text{ at.}^{-1}$, i.e. $(4.8 \pm 0.7) \times 10^{20} \text{ cm}^{-3}$, was found in H-plasma treated crystal in a subsurface layer at a depth of 100 nm. Hence although a significant enhancement of H concentration was detected in the subsurface layer, the H concentration in the bulk is still comparable to that in the virgin sample within the precision of NRA ($2 \times 10^{-4} \text{ at.}^{-1}$). Since the process (iii) requires diffusion of a certain fraction of H from the sub-surface layer into the bulk, it is important to estimate the H concentration required for the conversion of $V_{Zn}+1H$ complexes into $V_{Zn}+2H$ and compare it with the NRA detection limit. The

concentration of $V_{Zn}+1H$ complexes in the virgin HTG ZnO crystal estimated by Eq. (3) is $c_{V_{Zn}+1H} \approx 2 \times 10^{-4} \text{ at.}^{-1}$. Thus, hydrogen concentration of $2 \times 10^{-4} \text{ at.}^{-1}$, which is just the NRA detection limit, is sufficient to fill all of $V_{Zn}+1H$ complexes and convert them into $V_{Zn}+2H$. This indicates that a conversion of some $V_{Zn}+1H$ defects into $V_{Zn}+2H$ complexes - invisible to positrons - may occur not only in the sub-surface layer, but also deeper in the bulk and this is not in contradiction with the NRA results that virtually no increase in H concentration in the volume of the H-plasma treated crystal is detected. This estimate further supports the picture that the processes (i) and (ii) are likely to operate simultaneously in H-plasma treated crystals.

Crystal surface quality. The surface quality of the single crystals was checked before and after the H-plasma treatment by AFM, and results representative of both crystals are shown in Fig. 4. The virgin HTG ZnO single crystal revealed three height levels of micro-plateaus with a coverage of 75%, 20%, and 5% for the lowest, medium, and highest level, respectively (Fig. 4a). The corresponding cross section image (Fig. 4b) reveals nearly constant height steps between the micro-plateaus amounting to 4 nm which is about eight times the c -lattice constant of ZnO.

After the sample treatment in remote H-plasma a kind of reconstruction of the surface, namely the loss of the three clearly separated height levels and of the micro-plateaus, was observed (Fig. 4d). From the cross section line (Fig. 4c) the formation of nano-crystallites with diameters ranging between 50 and 150 nm and a height ranging between 4 and 25 nm was observed. The depth distribution of nano-crystallites (Fig. 4c) ranges between 10 and 15 nm. These nano-crystallites manifest themselves as the very narrow sub-surface region 'layer 1' observed by SPIS in both crystals, characterized by the very short $L_+ \leq 1 \text{ nm}$ [6]. Moreover, a long-lived positron lifetime component $\tau_3 \sim 1\text{-}3 \text{ ns}$ was detected in this layer by PLEPS [6]. It is striking to note that this longest component is almost entirely found near the sample surface with an intensity of $\sim 3 \%$ or less. This suggests that it is associated with formation of o-Ps at inter-granular open volumes among the nano-crystallites observed by AFM at both sample surfaces. Formation of nano-crystallites in the sub-surface layer indicates mass transport in H-plasma treated crystals. This is in accordance with formation of nano-voids and diffusion of Zn_i into ZnO bulk. Hence, surface modifications revealed by AFM indicate that in addition to the processes (i) and (iii) also the process (ii) takes place during H-plasma treatment.

SRIM [9] calculations were performed to simulate the bombardment of ZnO by 400 eV H ions. These simulations show that such ions may reach depths of $\sim 20 \text{ nm}$, with a distribution peaked at $(7.4 \pm 0.4) \text{ nm}$. Furthermore, about 0.1 vacancies per impinging ion are produced in total (SRIM does not differentiate between Zn and O vacancies). Thus, the surface modification observed by AFM clearly correlates with the bombardment of H ions from the remote plasma due to the bias of -330 V applied to the sample.

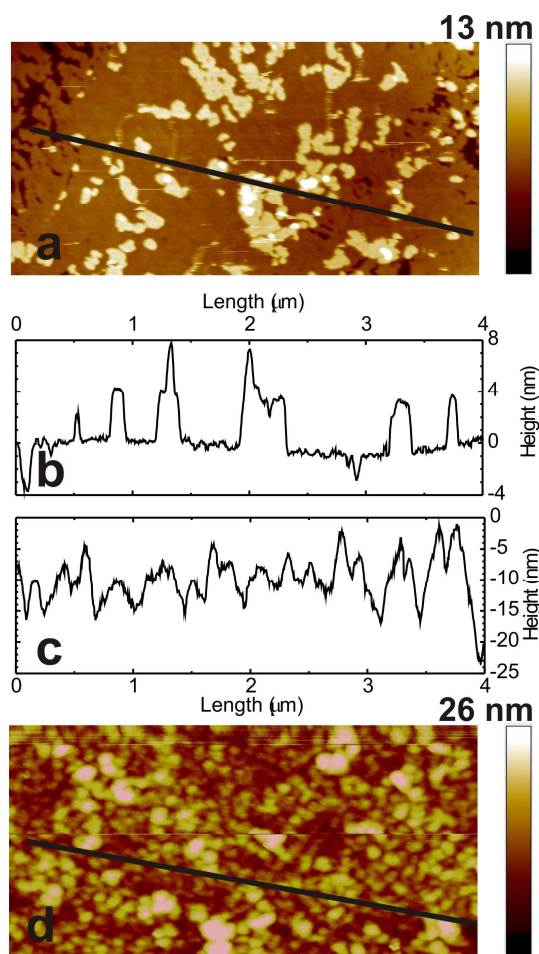


Figure 4 AFM scans ($4 \times 2 \mu\text{m}$) recorded on a HTG ZnO single crystal before (a) and after (d) remote H-plasma treatment. The roughness in the $4 \times 2 \mu\text{m}$ scan area amounts to 1.7 nm (a) and 4.8 nm (d). The $4 \mu\text{m}$ long section lines have been taken along the black lines in the corresponding AFM scans and reveal the micro-plateaus before (b) and after (c) remote H plasma treatment.

Summary

Structure investigations of HTG ZnO single crystals, before and after treatment in remote H-plasma treatment were performed by PAS combined with AFM investigations. From AFM it has been found that the H-plasma treatment results in a surface modification, i.e. the formation of a narrow nano-crystalline surface layer, which can clearly be correlated with the bombardment of energetic H ions as seen from SRIM calculations. PAS investigations gave evidence that the concentration of positron traps in the volume of the H-plasma treated crystals was lowered and thus some fraction of positrons annihilate from a free state. Observed decrease in concentration of positron traps in H-plasma treated ZnO crystals is caused by several processes: (i) thermally activated mutual annihilation of $V_{\text{Zn}}+1\text{H}$ complexes with Zn_i existing in the sample, (ii) H-plasma assisted diffusion of Zn_i into the bulk and filling the $V_{\text{Zn}}+1\text{H}$ complexes, and (iii) trapping of H atoms in $V_{\text{Zn}}+1\text{H}$ leading to the formation of $V_{\text{Zn}}+n\text{H}$ ($n > 2$) complexes which do not trap positrons. Results of CDB and AFM measurements strongly indicate that all processes (i) – (iii) take place simultaneously during H-plasma treatment of ZnO crystals.

Acknowledgement

We are thankful to F. Börrnert (TU Dresden) for his careful treatment of the ZnO samples in remote H plasma. This work was supported by the Czech Science Foundation (project No. P108/11/0958) and the Ministry of Schools, Youths and Sports of the Czech Republic (project No. 0021620834).

References

- [1] G. Brauer, W. Anwand, D. Grambole, J. Grenzer, W. Skorupa, J. Čížek, J. Kuriplach, I. Procházka, C.C. Ling, C.K. So, D. Schulz, D. Klimm, *Phys. Rev. B* 79 (2009) 115212.
- [2] Z.Q. Chen, S.J. Wang, M. Maekawa, A. Kawasuso, H. Naramoto, X.L. Yuan, T. Sekiguchi, *Phys. Rev. B* 75 (2007) 245206.
- [3] F. Tuomisto, D.C. Look, *Proc SPIE* 6474 (2007) 647413.
- [4] C.G. Van de Walle, *Phys. Rev. Lett.* 85 (2000) 1012.
- [5] A. Janotti, C.G. Van de Walle, *Nature Mater.* 6 (2007) 44.
- [6] W. Anwand, G. Brauer, T.E. Cowan, D. Grambole, W. Skorupa, J. Čížek, J. Kuriplach, I. Procházka, W. Egger, P. Sperr *Phys. Status Solidi A* 207 (2010) 2415.
- [7] W. Anwand, G. Brauer, T.E. Cowan, V. Heera, H. Schmidt, W. Skorupa, H. von Wenckstern, M. Brandt, G. Benndorf, M. Grundmann *Phys. Status Solidi A* 207 (2010) 2426.
- [8] W.A. Lanford, *Handbook of Modern Ion Beam Materials Analysis*, ed. R. Tesmer, M. Nastasi, Materials Research Society, Pittsburg, 1995.
- [9] J.F. Ziegler, J.P. Biersack, U. Littmark, *The Stopping and Range of Ions in Solids*, Pergamon, New York 1985.
- [10] F. Bečvář, J. Čížek, I. Procházka, J. Janotová, *Nucl. Instrum. Methods A* 539 (2005) 372.
- [11] F. Bečvář, J. Čížek, I. Procházka, *Appl. Surf. Sci.* 255 (2008) 111.
- [12] F. Bečvář, *Nucl. Instrum. Methods B* 261 (2007) 871.
- [13] I. Procházka, I. Novotný, F. Bečvář *Mater. Sci. Forum* 255-257 (1997) 772.
- [14] J. Čížek, I. Procházka, B. Smola, I. Stulíková, R. Kužel, Z. Matěj, V. Cherkaska, *Phys. Stat. Sol. a* 203 (2006) 466
- [15] M.J. Puska, R.M. Nieminen, *J. Phys. F: Met. Phys.* 13 (1983) 333.
- [16] B. Barbiellini, M.J. Puska, T. Korhonen, A. Harju, T. Torsti, R.M. Nieminen, *Phys. Rev. B* 53 (1996) 16201.
- [17] I. Makkonen, M. Hakala, M.J. Puska, *Phys. Rev. B* 73 (2006) 035103.
- [18] J. Kuriplach, A.L. Morales, C. Dauwe, D. Segers, M. Šob, *Phys. Rev. B* 58 (1998) 10475.
- [19] M. Mizuno, H. Araki, Y. Shirai, *Mater. Trans.* 45 (2004) 1964.
- [20] R.N. West, in: P. Hautojärvi (Ed.), *Positrons in Solids*, Springer-Verlag, Berlin, 1979, pp. 89.
- [21] G. Brauer, W. Anwand, W. Skorupa, J. Kuriplach, O. Melikhova, C. Moisson, H. von Wenckstern, H. Schmidt, M. Lorenz, M. Grundmann, *Phys. Rev. B* 74 (2006) 045208.
- [22] W. Anwand, G. Brauer, R.I. Grynszpan, T.E. Cowan, D. Schulz, D. Klimm, J. Čížek, J. Kuriplach, I. Procházka, C.C. Ling, A.B. Djurišić, V. Klemm, G. Schreiber, D. Rafaja, *J. Appl. Phys.* 109 (2011) 063516.
- [23] R. Krause-Rehberg, H.S. Leipner, *Positron Annihilation in Semiconductors – Defect Studies*, Springer, Berlin 1999.
- [24] A. Uedono, T. Koida, A. Tsukazaki, M. Kawasaki, Z.Q. Chen, S. Chichibu, H. Koinuma, *J. Appl. Phys.* 93 (2003) 2481.
- [25] T. Koida, S.F. Chichibu, A. Uedono, A. Tsukazaki, M. Kawasaki, T. Sota, Y. Segawa, H. Koinuma, *Appl. Phys. Lett.* 82 (2003) 532.

-
- [26] A. Zubiaga, F. Tuomisto, F. Plazaola, K. Saarinen, J.A. Garcia, J.F. Rommeluere, J. Zuniga-Perez, V. Munoz-Sanjose, *Appl. Phys. Lett.* 86 (2005) 042103.
- [27] K.H. Tam, C.K. Cheung, Y.H. Leung, A.B. Djurisic, C.C. Ling, C.D. Beling, S. Fung, W.M. Kwok, W.K. Chan, D.L. Phillips, L. Ding, W.K. Ge, *J. Phys. Chem. B* 110 (2006) 20865.
- [28] B. Nielsen, K. G. Lynn, A. Vehanen, P. J. Schultz, *Phys. Rev. B* 32 (1985) 7561.
- [29] A. Uedono, L. Wei, Y. Tabuki, H. Kondo, S. Tanigawa, K. Wada, H. Nakanishi, *Jpn. J. Appl. Phys., Part 2* 30 (1991) L2002.
- [30] R.A. Rabadanov, M.K. Guseikhanov, I. Sh. Aliev, S.A. Semilov, *Izvestiya Vysshikh Uchebnykh Zavedenii, Fizika* 6 (1981) 72.
- [31] N. Tomiyama, M. Takenaka, E. Kuramoto, *Mater. Sci. Forum* 105-110 (1992) 1281.
- [32] S. Zh. Karazhanov, E.S. Marstein, A. Holt *J. Appl. Phys.* 105 (2009) 033712.
- [33] J. Čížek, N. Žaludová, M. Vlach, S. Daniš, J. Kuriplach, I. Procházka, G. Brauer, W. Anwand, D. Grambole, W. Skorupa, R. Gemma, R. Kirchheim, A. Pundt, *J. Appl. Phys.* 103 (2008) 053508.

Near-Surface Depth Profiling of Solids by Mono-Energetic Positrons

10.4028/www.scientific.net/DDF.331

Characterization of H-Plasma Treated ZnO Crystals by Positron Annihilation and Atomic Force Microscopy

10.4028/www.scientific.net/DDF.331.113